Human Pathology (2020) **103**, 72–82

ELSEVIER

Human PATHOLOGY

www.elsevier.com/locate/humpath

Original contribution

Immunohistochemical distinction of paragangliomas from epithelial neuroendocrine tumors—gangliocytic duodenal and cauda equina paragangliomas align with epithelial neuroendocrine tumors☆,☆☆

Divya Mamilla MD [a], Irena Manukyan MD [b], Patricia A. Fetsch MT, ASCP [b], Karel Pacak MD [a], Markku Miettinen MD [b,*]

[a] *Section on Medical Neuroendocrinology, Eunice Kennedy Shriver National Institute of Child, Health and Human Development, National Institutes of Health, Bethesda, MD, 20892, USA*
[b] *National Cancer Institute, Laboratory of Pathology, Bethesda, MD, 20892, USA*

Received 10 June 2020; revised 6 July 2020; accepted 7 July 2020

Available online 12 July 2020

Keywords:
Paraganglioma;
Neuroendocrine tumor;
GATA3;
Keratins;
Tyrosine hydroxylase;
Gangliocytic paraganglioma;
Cauda equina paraganglioma

Summary Distinction of paraganglioma (PGL) from epithelial neuroendocrine tumors (NETs) can be difficult as they can mimic each other by nested architecture and expression of neuroendocrine markers. In this study, we examined differential diagnostic markers in 262 PGLs (142 adrenal pheochromocytomas and 120 extra-adrenal PGLs), 9 duodenal gangliocytic PGLs and 3 cauda equina PGLs, and 286 NETs (81 GI, 78 pancreatic, 42 thoracic, 37 medullary thyroid carcinomas, and 48 high-grade NETs including 32 small cell carcinomas of lung). While keratin expression was nearly uniform in NETs with the exception of few tumors, extensive keratin expression was seen in only one PGL (<1%) and focal expression in 5% PGLs. GATA3 was present in >90% of PGLs but only in 2% of NETs, usually focally. Tyrosine hydroxylase (TH) was expressed in >90% of adrenal, abdominal, and thoracic PGLs but only in 37% of head and neck PGLs, reflecting their variable catecholamine synthesis. Focal or occasional extensive TH-expression was detected in 10% of NETs. CDX2 was a helpful discriminator seen in 28% of pancreatic and most GI NETs but in no PGLs. SOX10 detected sustentacular cells in 85% of PGLs and 7% of NETs, whereas GFAP detected sustentacular cells mainly in PGLs of neck and was absent in NETs. Duodenal gangliocytic PGLs (n = 9) and all cauda equina PGLs (n = 3) expressed keratins, lacked GATA3, showed no or minimal TH expression as some NETs, and contained SOX10 and S100 protein-positive spindle cells negative for GFAP. Ganglion-like epithelioid cells were keratin-positive and negative for TH and SOX10 differing from true ganglion cells. We conclude that duodenal gangliocytic and cauda equina PGLs have a NET-

☆ Competing interests: The authors have no conflicts of interest to disclose.
☆☆ Funding/Support: Supported by NIH's intramural Research Program.

* Corresponding author. Laboratory of Pathology, NCI/NIH, 9000 Rockville Pike, Bldg. 10, Rm. 2S235C, Bethesda, Maryland 20892, USA.
E-mail address: miettinenmm@mail.nih.gov (M. Miettinen).

https://doi.org/10.1016/j.humpath.2020.07.010
0046-8177/Published by Elsevier Inc.

like immunoprofile and differ from ordinary PGLs. NETs can be distinguished from PGLs by their expression of keratins and general lack of GATA3, TH, and GFAP-positive sustentacular cells, and sometimes by expression of CDX2 or TTF1.
Published by Elsevier Inc.

1. Introduction

Adrenal pheochromocytoma, the most common paraganglioma (PGL), and other PGLs are nonepithelial neuroendocrine neoplasms derived from chromaffin cells of the adrenal medulla and paraganglia of the sympathetic and parasympathetic nervous systems. They can occur in locations where paraganglia normally reside and as metastases almost at any site [1,2]. The histologic diagnosis of PGLs is straightforward when tumor involves a common site and has a typical histology with a nested architecture. However, epithelial neuroendocrine tumors (NETs), such as carcinoids, pancreatic NETs, thyroid medullary carcinoma, and high-grade neuroendocrine carcinomas, can also have nested patterns and mimic PGLs. Small specimens can be problematic as architectural landmarks can be limited. In these instances, immunohistochemistry is necessary for this clinically important distinction.

Both PGLs and NETs typically express pan-neuroendocrine markers chromogranin A, synaptophysin, and insulinoma-associated protein 1 (INSM1) [1,3,4]. Therefore, other markers are necessary for immunohistochemical distinction of PGLs from NETs.

Keratin monoclonal antibody cocktail AE1/AE3 detects nearly all soft epithelial (nonhair) keratins, except keratins 10, 17, and 18 [5]. It is therefore expected to be positive in all epithelial NETs. Keratin antibody CAM5.2 detects specifically keratin 8 [6]. Keratins have been occasionally reported in conventional PGLs (of adrenal, retroperitoneum, urinary bladder, carotid body, and thorax) [7,8].

GATA3 (GATA-binding protein 3 and transacting T-cell−specific factor) is one of the 6 members of dual zinc-finger transcription factors that binds to the DNA sequence GATA. It is essential in neuronal embryogenesis regulating the expression of the noradrenergic factor tyrosine hydroxylase (TH) and differentiation and survival of neurons and chromaffin cells [9]. GATA3 has been reported in PGLs and generally absent in NETs but has not been studied in gangliocytic and cauda equina PGLs [10−12].

TH, the rate limiting enzyme involved in conversion of L-tyrosine to L-DOPA, has been detected biochemically and immunohistochemically in PGLs and in sporadic NETs, but it has not been extensively studied in NETs [13−15].

Organ-specific transcription factors, such as thyroid transcription factor 1 (TTF1) and caudal type homeobox 2 (CDX2), and hormonal markers can be useful in characterization of NETs, but none of them is universal for all subgroups [16,17]. TTF1 has been studied in PGLs of thorax but not at other sites. CDX2 has been detected in some pancreatic NETs [16] but has not been studied in PGLs.

Sustentacular cells, elongated, slender spindle cells variably outlining the cell nests of PGLs have also been detected in some NETs. They can be highlighted by immunostains for S100 protein, glial fibrillary acidic protein (GFAP), and SOX10 [18−21]. However, these have not been systematically studied in large sets of NETs and PGLs of various sites.

Gangliocytic PGL is a rare NET containing ganglion-like cells and typically occurring in the 2nd part of duodenum. It differs from conventional PGL by common keratin expression [22,23]. Neither it nor cauda equina PGL, another rare type of keratin-expressing PGL occurring in the caudal neural tube [24], has been studied for GATA3 and TH.

In this study, we examined the expression 5 groups of markers comparatively in >500 PGLs and NETs of various sites in special groups of rare PGLs: gangliocytic PGL of duodenum and cauda equina PGL.

2. Materials and methods

A large group (n = 560) of NETs was examined histologically to confirm the diagnosis and arranged in manually prepared multitumor blocks as described before [25]. A small number of cases were studied using whole sections. The cases originated from 1970 to 2019 and were de-identified having sparse annotations for tumor site, size, patient age, sex, and a possible germline tumor syndrome. These tumors included 262 PGLs: 142 adrenal and 120 extra-adrenal examples, including 54 cervical, 49 retroperitoneal, 9 thoracic, and 8 urinary bladder PGLs. Approximately 40% of PGLs were germline syndrome-associated tumors (RET, VHL, SDH subunits, and NF1). There were also 9 duodenal gangliocytic PGLs and 3 cauda equina PGLs. The 286 epithelial NETs included 81 grade 1−2 intestinal and 42 pulmonary NETs/carcinoids, 78 pancreatic NETs, and 37 medullary carcinomas of thyroid. High-grade (grade 3) NETs included 32 small cell carcinomas of lung and 16 high-grade neuroendocrine carcinomas of various sites (4 pulmonary large cell, 4 gastrointestinal, 2 endometrial, 1 sinonasal, 1 urinary bladder, and 4 metastatic tumors of unknown origin).

Table 1 Antibodies and immunohistochemical protocols used in the study.

Antibody	Source	Clone	Dilution	Automation	Epitope retrieval/time (min)	Primary antibody incubation time (min)	Detection
CDX2	Roche	EPR2764Y	Predilute	Roche	CCI 64	36	UltraView with amplification + DAB
Chromo-Granin A	Roche	LK2H10	Predilute	Roche	CC1 36	20	UltraView + DAB
GATA3	Roche	L50-823	Predilute	Roche	CC1 64	60	UltraView + DAB
GFAP	Roche	EP672Y	Predilute	Roche	CC1 64	32	UltraView + DAB
INSM1	Santa Cruz	A-8	1:1000	Leica	ER2 25	30	Bond Polymer Refine + DAB
Keratins AE1/3	Dako Agilent	AE1+AE3	1:100	Roche	CC1 36	32	UltraView + DAB
Keratin 8	Roche	CAM5.2	Predilute	Roche	Protease 1, 8 min	20	UltraView + DAB
PNMT	Novus Biologicals	OTI1D2	1:400	Leica	ER2 25	30	Bond Polymer Refine + DAB
S100 protein	Biogenex	15E2E2	1:8000	Roche	CC1 64	32	UltraView + DAB
SOX10	Cell Marque	EP268	1:100	Roche	CC1 64	32	UltraView + DAB
Synaptophysin	Roche	SP11	Predilute	Roche	CC1 64	32	UltraView with amplification + DAB
TTF1	Roche	SP141	Predilute	Roche	CC1 64	20	UltraView with block
Tyrosine hydroxylase	Abcam	EP1532Y	1:3000	Leica	ER2 25	30	Bond Polymer Refine + DAB

Abbreviations: CDX2, caudal type homeobox 2; INSM1, insulinoma-associated protein 1; PNMT, phenylethanolamine N-methyl transferase; TTF1, thyroid transcription factor 1; GATA3, GATA-binding protein 3 and transacting T-cell−specific factor.

Immunohistochemical studies were performed by automated systems (Ventana Bench-mark Ultra or Leica Bond). Antibodies and protocols are listed in Table 1. All tumors were confirmed immunopositive for at least 1, usually all 3 neuroendocrine markers, chromogranin A, synaptophysin, and INSM1 [1−4]. There was a slightly lower positivity for INSM1 in all tumor categories.

Immunohistochemical studies for keratins (AE1/AE3 cocktail, keratin 8: CAM5.2), transcription factors (GATA3, CDX2, and TTF1), and TH were tabulated in detail for estimated percentage of positive tumor cells. Expression of markers for sustentacular cells (S100 protein, GFAP, and SOX10) were evaluated in a 0−3 scale for the area of 40x magnification richest on these cells as follows: 0 = no positive cells, 1 = 1−10 cells, 2 = 11−49, 3 ≥ 50 cells. As the results from S100 protein expression in sustentacular cells were generally similar to those of SOX10 and there was variable labeling of chief cells/neuroendocrine cells for S100 protein, results of only SOX10 were tabulated. Expression of phenyl-ethanolamine N-methyltransferase was also studied in >500 PGLs and NETs. While the results were partly similar to those of TH, they were more difficult to interpret as many NETs showed diffuse weak expression, and PGLs showed variable and unpredictable expression. Therefore, this marker was not examined further.

3. Results

The immunohistochemical results have been summarized in Table 2.

3.1. Conventional paragangliomas

These tumors included pheochromocytomas, retroperitoneal (usually paraaortic or aortocaval), thoracic/aorticopulmonary, urinary bladder, and neck PGLs (most from the carotid body, one from larynx, and one from the higher neck).

Most PGLs were negative for keratins AE1/AE3 and keratin 8 (CAM5.2). Exceptional, extensive AE1/AE3 and keratin 8-positivity was seen in one pheochromocytoma in approximately 80% of tumor cells, whereas this tumor was positive for GATA3 and TH typical of PGLs (Fig. 1). Focal keratin expression with both antibodies was detected in ≤5% of tumor cells in 12 conventional PGLs, 0−7% in various subgroups, and these cells had a thin, slender morphology, consistent with sustentacular cells (Table 2).

GATA3 nuclear expression was seen in most pheochromocytomas, PGLs of abdomen, thorax, and head and neck, usually extensively. Some cases showed zonal expression patterns probably associated with suboptimal antigen preservation. The negative cases included a small subset PGLs of different sites (Table 2).

Table 2 Summary of marker expression in 560 paragangliomas and epithelial neuroendocrine tumors.

Tumor category	n	Keratins AE1/AE3	GATA3		Tyrosine hydroxylase positive cells		CDX2	TTF1	SOX10[b] 0/1/2/3	GFAP[b] 0/1/2/3
Pheochromocytoma, adrenal	142	8/142[a]	132/142	(93)	138/142	(97)	0/145	2/142[a]	30/33/35/26	109/4/1/1
Paraganglioma, retroperitoneal	49	3/49[a]	46/49	(94)	43/49	(88)	0/48	0/48	4/11/18/12	44/1/0/0
Paraganglioma, urinary bladder	8	0/8	6/8	(75)	8/8	(100)	0/6	0/6	0/2/1/3	All negative
Paraganglioma, neck	54	1/54[a]	51/54	(93)	20/54	(37)	0/54	0/54	3/2/19/30	14/12/14/14
Paraganglioma, thoracic	9	0/9	9/9	(100)	9/9	(100)	0/9	0/9	1/0/0/7	3/2/1/2
Gangliocytic paraganglioma	9	9/9	0/9	(0)	2/9[a]	(22)	0/9	0/9	9/9 [b]	All negative
Cauda equina paraganglioma	3	3/3	0/3	(0)	2/3[a]	(0)	0/2	0/2	0/2/0/0	All negative
Carcinoid/NET,GI-tract, Gr.1-2	81	81/81	0/81	(0)	6/81[a]	(7)	73/81	0/81	79/2/0/0	81/0/0/0
Carcinoid/NET, lung and thymus, Gr. 1−2	42	42/42	1/42[a]	(2)	11/42[a]	(26)	0/41	19/41	28/7/4/2	All negative
NET, pancreas, Gr. 1-2	78	76/78	5/77[a]	(6)	7/77[a]	(9)	22/78	1/78	74/4/1/0	All negative
Medullary carcinoma, thyroid	37	37/37	0/37	(0)	1/37[a]	(2)	0/37	37/37	37/0/0/0	All negative
Neuroendocrine tumor, Gr. 3, Various organs	16	15/16	0/16	(0)	2/16[a]	(13)	8/16	7/16	16/0/0/0	All negative
Small cell carcinoma, lung	32	30/32	0/31	(0)	0/32	(0)	0/30	30/32	30/0/0/0	ND
Total	560									

Note. Number of cases with each score value (Number of positive cells per 0.2 mm^2, Scored 0−3: 0 = negative, 1 = ≤10, 2 = 11−49, 3 = ≥50). Numbers for SOX10 and GFAP represent the cases with no positivity (Score 0) to ≥50 cells positive (Score 3). Details of scoring for SOX10 and GFAP are shown in materials and methods.

Abbreviations: CDX2, caudal type homeobox 2; NET, neuroendocrine tumor; TTF1, thyroid transcription factor 1; GATA3, GATA-binding protein 3 and transacting T-cell−specific factor.

[a] Positivity was usually focal.

[b] Expression only in sustentacular cells/spindled Schwannian cells.

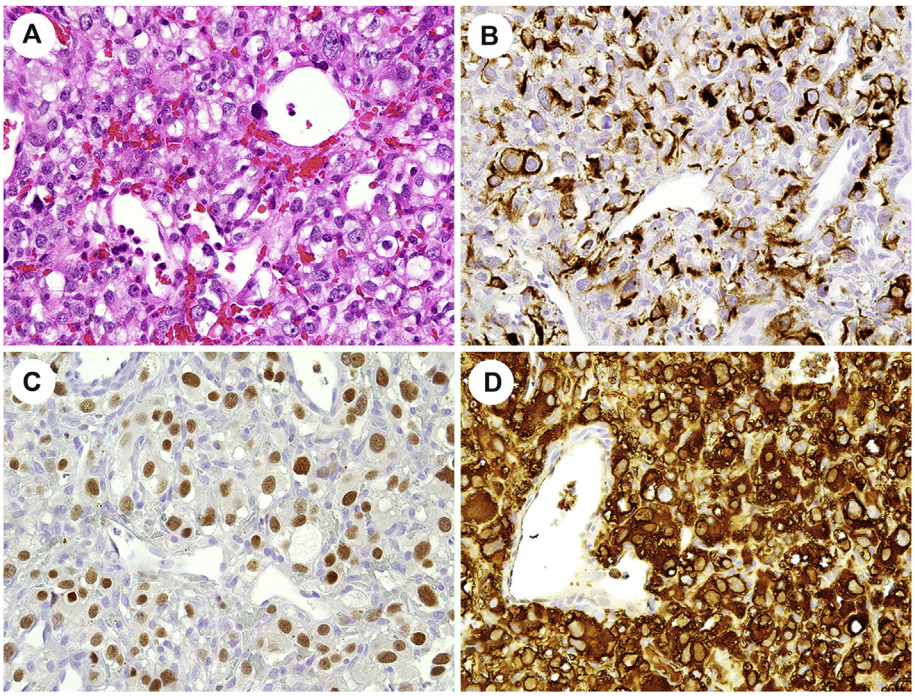

Fig. 1 A, Para-aortic paraganglioma is composed of clear or eosinophilic epithelioid cells. B, Most tumor cells in this case show exceptional positivity for keratin cocktail AE1/AE3. C, Tumor cells have nuclear positivity for GATA3. D, Tumor is strongly positive for tyrosine hydroxylase.

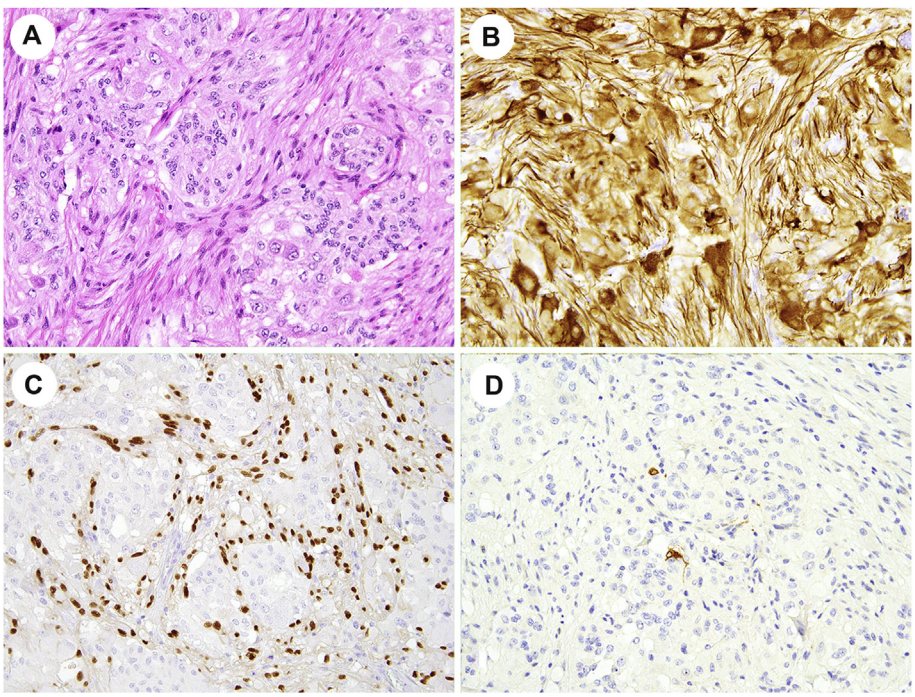

Fig. 2 A, Gangliocytic paraganglioma of duodenum is composed of nests of epithelioid cells containing ganglion-like cells and Schwannian stroma between nests. B, The epithelioid cells including the ganglion-like cells are positive for keratin 8 (CAM5.2), which also highlights thin cell processes. C, The Schwannian stromal cells are positive for SOX10, whereas the epithelioid cells are negative. D, Only few tumor cells are tyrosine hydroxylase positive.

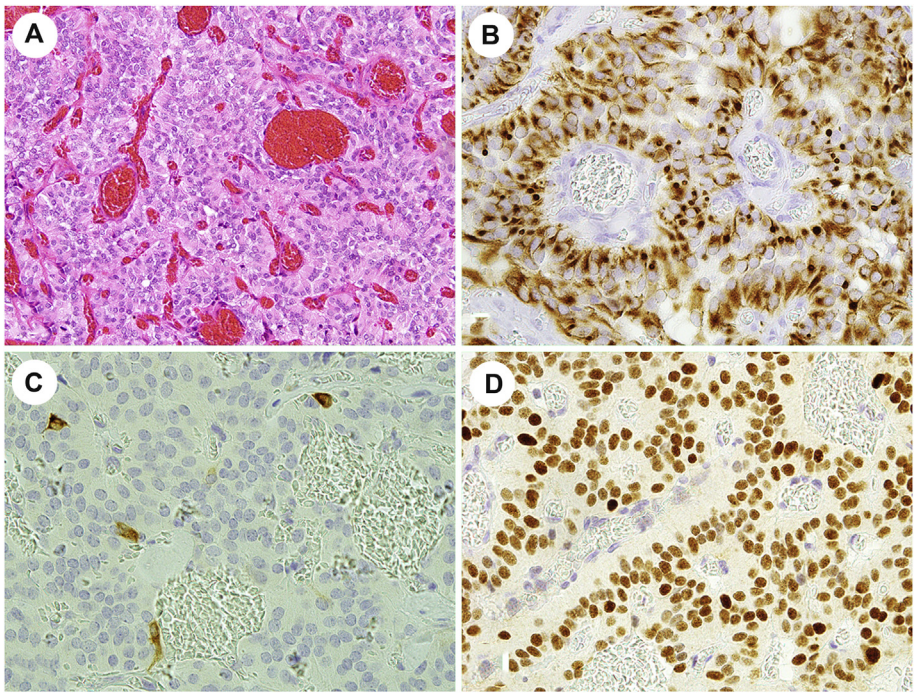

Fig. 3 A, Cauda equina paraganglioma is a highly vascular tumor composed of epithelioid cells with perivascular arrangements. B, Tumor is positive for keratins AE1/AE3. C, Few scattered tumor cells are positive for tyrosine hydroxylase. D, Like most neuroendocrine tumors, this one shows nuclear positivity for INSM1. INSM1, insulinoma-associated protein 1.

TH was nearly always extensively expressed in the cytoplasm of adrenal, retroperitoneal, thoracic, and urinary bladder PGLs (88−98%). However, PGLs of the neck were heterogeneous showing positivity in only 20/54 cases (37%). Nerves and ganglion cells were also positive. CDX2 was expressed in none of the conventional PGLs. TTF1 was focally expressed in 2 adrenal PGLs in <5% of tumor cells.

SOX10-positive sustentacular cells were variably present in PGLs. They were numerous in most PGLs of the neck and thorax and scant or absent in adrenal, urinary bladder, and retroperitoneal PGLs (Table 2). GFAP-positive sustentacular cells were predominantly detected in PGLs of the head and neck and thorax. In adrenal, urinary bladder, and retroperitoneal PGLs, they were usually absent or present only in small numbers (Table 2). SOX10 or GFAP did not label chief cells in any PGLs or NETs.

While S100 protein and SOX10 showed identical distribution in sustentacular cells, S100 protein also labeled chief cells in 50−70% PGLs of different sites, 65% of pancreatic NETs, 10% of pulmonary NETs, but only 2% of GI NETs.

3.2. Gangliocytic and cauda equina paragangliomas

The 9 gangliocytic PGLs occurred in 4 females and 4 males aged 42−74 years (median, 65 years). Demographic information was unavailable in 1 case. All tumors were duodenal submucosal polypoid masses measuring 1.5−5 cm.

These tumors had neuroendocrine nests containing scattered ganglion-like cells. Mitotic activity was <2/10 high power fields (HPFs) in all cases, equivalent to NET grade 1. The nests were surrounded by a variably prominent spindle cell component. The nests of epithelioid neuroendocrine cells, including ganglion-like cells with abundant cytoplasm and angulated outlines, were also positive for keratins AE1/AE3 and more extensively positive for keratin 8 (CAM5.2), which also highlighted delicate cell processes of the epithelial cells (Fig. 2). All gangliocytic PGLs were negative for GATA3, CDX2, and TTF1. Only minimal TH-positivity (<2% of tumor cells) was detected in 2 cases, whereas the remaining cases were negative. The ganglion-like cells were negative for TH, GATA3, and SOX10, thus differing from ordinary ganglion cells. The spindle cells between the neuroendocrine nests were positive for S100 protein and SOX10, consistent with their Schwannian nature (Fig. 2), and were negative for GFAP.

The 3 cauda equina PGLs were diffusely positive for keratins AE1/AE3 and negative for GATA3. Two of the cases studied for keratin 8 were also positive. Focal TH positivity was seen in 2 cases (Fig. 3). A small number of SOX10-positive cells were present with no GFAP-positive cells in the 2 cases tested that were also negative for CDX2 and TTF1.

Table 3 Epithelial neuroendocrine tumors and paragangliomas with aberrant results on expression of keratins, GATA3, or tyrosine hydroxylase potentially challenging the original classification. The number under an immunomarker is the estimated percentage of positive tumor cells.

Case	Starting diagnosis	Age/Sex	Size	Ker AE1+AE3/keratin 8	GATA3	Tyrosine hydroxylase	CDX2	TTF1	Score of SOX10/GFAP	Conclusion
1	NET, pancreas, Grade 1	65 F	7.5 cm	0/0	100	0	0	0	2/0	Probable (peri)pancreatic paraganglioma, negative for keratins
2	NET, pancreas, Grade 1	58 F	unk	0/0	0	60	100	0	0/0	Probable pancreatic NET, positive for TH and CDX2
3	NET, pancreas, Grade 1	45 M	7.5 cm	100/100	80	0	0	0	0/0	Pancreatic NET with extensive GATA 3-positivity
4	NET, pancreas, Grade 2	59 F	7 cm	100/100	20	0	0	0	0/0	Pancreatic NET with GATA 3-positivity
5	NET, pancreas Grade 1	67 F	5.5 cm	100/100	0	80	0	0	0/0	Pancreatic NET with TH-positivity
6	NET, pancreas Grade 1	69 F	unk	70/100	0	100	90	0	1/0	Pancreatic NET with TH-positivity
7	NET, lung, Grade 1	65 F	unk	5/100	0	30	0	0	0/0	NET of lung with low keratin AE1/AE3 and TH-positivity
8	NET, lung, Grade 2	69 M	unk	20/100	0	10	0	0	0/0	NET of lung with low keratin AE1/AE3 and focal TH-positivity, TTF1-negative
9	NET, lung, Grade 1	18 F	2.5 cm	5/100	0	60	0	0	1/0	NET of lung with low keratin and extensive TH-positivity, TTF1-negative
10	NET, lung, Grade 1	61 F	2.2 cm	80/100	0	20	0	100	0/0	NET of lung with TH-positivity
11	Pheochromocytoma	34 M	1.8 cm	80/100	80	100	0	0	3/0	Pheochromocytoma with extensive keratin expression

Note. Scoring of SOX10 (left of/) and GFAP (right of/): 0 = negative; 1 = 1−10 cells per HPF, 2 = 11−49 cells per HPF, 3 = $\geq$ 50 cells per HPF.
Abbreviations: CDX2, caudal type homeobox 2; NET, neuroendocrine tumor; TH, tyrosine hydroxylase; TTF1, thyroid transcription factor 1; Unk, unknown; GATA3, GATA-binding protein 3 and transacting T-cell−specific factor.

3.3. Epithelial neuroendocrine tumors

All gastrointestinal, pancreatic, and pulmonary/mediastinal NETs and medullary thyroid carcinomas were extensively positive for keratins AE1/AE3 and keratin 8 (CAM5.2). Only 3% of NETs showed significantly higher labeling for keratin 8 than the AE1/AE3 cocktail. While most high-grade neuroendocrine carcinomas showed uniform keratin-positivity, 2 small cell carcinomas of lung were negative for both keratin antibodies (Table 2).

All gastrointestinal NETs were negative for GATA3, but 5 NETs of pancreas and 1 pulmonary carcinoid focally expressed GATA3 (Tables 2 and 3). Focal TH positivity was detected in gastrointestinal (6/81), pancreatic (7/77), and thoracic NETs (11/42), usually in <5% of tumor cells (Fig. 4). Occasional pancreatic NETs and pulmonary carcinoids showed more extensive TH-positivity (Fig. 4, Table 3). In some cases, pancreatic NETs with aberrant immunophenotypes, such as lack of keratins and strong TH expression, were CDX2-positive supporting the diagnosis of a pancreatic NET (Fig. 5).

Sustentacular cells with SOX10-positivity were rarely detected in NETs, essentially limited to thoracic and pancreatic NETs. GFAP-positive sustentacular cells were absent in all NETs (Table 2).

4. Discussion

PGLs and epithelial NETs from various organs can mimic each other because of their shared nested architecture and expression of pan-neuroendocrine markers chromogranin A, synaptophysin, and INSM1. Small specimens can be more challenging and require immunohistochemical support for diagnosis.

In this study, we examined >500 PGLs and NETs with a panel of 9 markers to evaluate their power in the distinction between these groups of NETs: (1) keratins AE1/AE3 and CAM5.2 (keratin 8), (2) transcription factors GATA3, CDX2, and TTF1, (3) TH, and (4) sustentacular cell markers S100 protein, SOX10, and GFAP.

Keratin-negativity of conventional PGL (excluding gangliocytic and cauda equina PGLs) is a useful parameter separating it from most NETs. However, 7% of PGLs did express keratins, but most of this expression was focal limited to sustentacular cells, and only 1 pheochromocytoma was extensively positive. Previous studies have also detected keratins in a small percentage of conventional PGLs [7,8].

TH, an enzyme involved in the biosynthesis of catecholamines, is expressed in neural tissue including paraganglia and has been detected especially in catecholamine

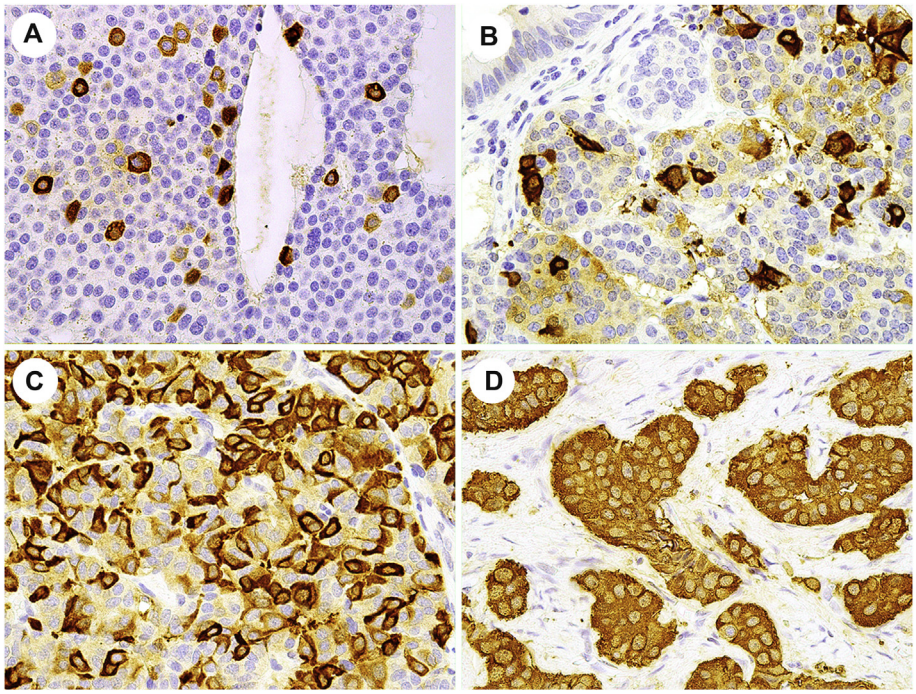

Fig. 4 Examples of tyrosine hydroxylase expression in epithelial neuroendocrine tumors. A, Ileal well-differentiated NET (carcinoid) shows a 1% cell population positive. B, Duodenal well-differentiated NET shows a small number of cells strongly positive and a larger proportion cells weakly positive. C, Well-differentiated NET (carcinoid) of lung contains 50% of positive cells. D, All tumor cells are positive for tyrosine hydroxylase in this unusual pancreatic NET. NET, neuroendocrine tumor.

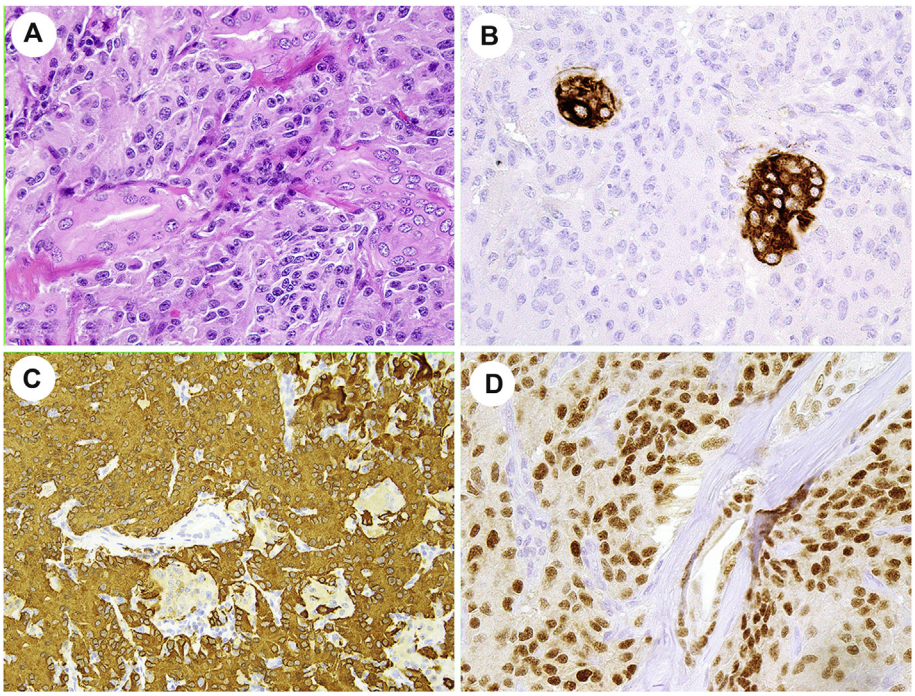

Fig. 5 Pancreatic NET mimicking paraganglioma. A, The tumor is composed of sheets of neuroendocrine cells between ductal elements. B, Tumor cells are negative for keratins AE1/AE3 (also negative for keratin 8/CAM5.2). C, Most tumor cells are positive for tyrosine hydroxylase. D, Tumor cells show nuclear positivity for CDX2 supporting the diagnosis of NET. NET, neuroendocrine tumor; CDX2, caudal type homeobox 2.

synthesizing PGLs and some carcinoids [14,15]. We confirmed nearly consistent TH expression in pheochromocytoma and abdominal and thoracic PGLs, whereas expression was far less common in neck/carotid body PGLs (32%); in a previous study, it was 27% [14]. We also found some TH expression in NETs, but this was usually focal and limited to scattered tumor cells. However, exceptions were noted with some NETs, especially pancreatic ones, being extensively TH-positive. TH has some value in distinguishing PGLs from NETs, but lack of its expression in most head and neck PGLs and extensive expression in some NETs are limitations.

Most PGLs including nearly all adrenal, retroperitoneal, thoracic, and neck/carotid body PGLs expressed GATA3, whereas NETs were negative making GATA3 a valuable marker in discrimination of PGLs from NETs as previously suggested [10–12]. However, our study reveals exceptions such as extensive GATA3 expression in 2% pancreatic and thoracic NETs, so that additional markers such as TH and transcription factors TTF1 and CDX2 could be used as further discriminators between NETs and PGLs. It should be considered in the differential diagnosis of NETs of head and neck that GATA3 is also expressed in parathyroid and pituitary adenomas [26,27]. Despite recently expressed concern about weaker GATA3-labeling of PGLs with immunohistochemistry protocols without robust epitope retrieval [28], we found that our 64-min epitope retrieval with Roche CC1 reagent and 60 min primary antibody incubation and UltraView detection gave a sufficient detection of GATA3 in PGLs (positivity >90% in all main subgroups).

While S100 protein-positive sustentacular cells are known in PGLs [1,20,21], they can also occur in some NETs [18,21]. We found that SOX10 is superior to S100 protein in enumerating sustentacular cells because it does not label the chief cells, as often seen in pulmonary and pancreatic NETs and PGLs of different sites. The common S100 protein-positivity in both PGLs and NETs should not lead to confusion with S100 positive neural or epithelial tumors.

The limitation in sustentacular cell evaluation is that they are abundant in only PGLs of head and neck and only variably present in adrenal and retroperitoneal PGLs. However, their presence in NETs is essentially limited to small subsets of pulmonary and pancreatic NETs. GFAP-positive sustentacular cells are restricted to PGLs of neck and thorax, which confirms a previous observation in a smaller number of PGLs [20]. The assessment of sustentacular cell populations has a limited value in the diagnosis of PGLs, although their absence has been suggested a possible but weak marker of malignancy (reviewed in Ref. [1]).

Aberrations in the main patterns of expression of keratins AE1/AE3, GATA3, and TH occurred mainly in pancreatic and pulmonary NETs (Table 3). The marker profile of one pancreatic NET indicated PGL-like differentiation: keratin and CDX2-negative and positive for

GATA3 and TH, supporting the diagnosis of a (peri) pancreatic PGL described in isolated reports [29,30]. However, there were also cases that in addition to keratin expression had strong expression of either GATA3 or TH raising the question whether there are pancreatic NETs with hybrid features of NET and PGL. Extensive genomic comparison could be useful to definitively determine the type of these tumors.

Our findings indicate that duodenal gangliocytic PGL and cauda equina PGLs align better with NETs than ordinary PGLs by their immunophenotype and should be classified as separate groups, perhaps termed as gangliocytic NET and cauda equina NET. In this study, all gangliocytic PGLs and cauda equina PGLs were extensively keratin-positive, negative for GATA3, and negative or minimally positive for TH, thus having an immunohistochemical profile similar to NETs, rather than conventional PGLs. A caveat is that there may be true spinal PGLs with classic PGL features different from cauda equina PGLs [31].

Ganglion-like cells in the epithelial islands of gangliocytic PGL seem to be keratin-positive and SOX10-negative epithelial neuroendocrine cells and not true ganglion cells. However, occurrence of entrapped normal ganglion cells in these tumors is possible.

Additional studies, such as extensive genomic sequencing and assessment of genomic methylation profiles, as now available for the diagnosis of brain tumors and sarcomas [32], might prove useful in determining the taxonomic status of gangliocytic and cauda equina PGLs among the NETs.

References

[1] Lack EE. Tumors of the adrenal glands and extraadrenal paraganglia. AFIP atlas of tumor pathology, fourth series; fasc 8. 2007. Washington, D.C: American Registry of Pathology in collaboration with the Armed Forces Institute of Pathology; 2007.

[2] Tischler AS, Asa SL. In: Mills SE, editor. Histology for pathologists. Philadelphia, PA: Wolters Kluwer; 2018.

[3] Rosenbaum JN, Guo Z, Baus RM, Werner H, Rehrauer W, Lloyd RV. INSM1: a novel immunohistochemical and molecular marker for neuroendocrine and neuroepithelial neoplasms. Am J Clin Pathol 2015;144:579–91.

[4] Mukhopadhyay S, Dermawan JK, Lanigan CP, Farver CF. Insulinoma-associated protein 1 (INSM1) is a sensitive and highly specific marker of neuroendocrine differentiation in primary lung neoplasms: an immunohistochemical study of 345 cases, including 292 whole-tissue sections. Mod Pathol 2019;32:100–9.

[5] Sun TT, Tseng SC, Huang AJ, Cooper D, Schermer A, Lynch MH, et al. Monoclonal antibody studies of mammalian epithelial keratins: a review. Ann N Y Acad Sci 1985;455:307–29.

[6] Kuruc N, Franke WW. Transient coexpression of desmin and cytokeratins 8 and 18 in developing myocardial cells of some vertebrate species. Differentiation 1988;38:177–93.

[7] Chetty R, Pillay P, Jaichand PV. Cytokeratin expression in adrenal phaeochromo-cytomas and extra-adrenal paragangliomas. J Clin Pathol 1998;51:477–8.

[8] Dermawan JK, Mukhopadhyay S, Shah AA. Frequency and extent of cytokeratin expression in paraganglioma: an immunohistochemical study of 60 cases from 5 anatomic sites and review of the literature. Hum Pathol 2019;93:16–22.

[9] Moriguchi T, Takako N, Hamada M, Maeda A, Fujioka Y, Kuroha T, et al. Gata3 participates in a complex transcriptional feedback network to regulate sympathoadrenal differentiation. Development 2006;133:3871–81.

[10] Sun TT, Tseng SC, Huang AJ, Cooper D, Schermer A, Lynch MH, et al. A study of gata3 and phox2b expression in tumors of the autonomic nervous system. Am J Surg Pathol 2013;37:1236–41.

[11] So JS, Epstein JI. GATA3 expression in paragangliomas: a pitfall potentially leading to misdiagnosis of urothelial carcinoma. Mod Pathol 2013;26:1365–70.

[12] Miettinen M, McCue PA, Sarlomo-Rikala M, Rys J, Czapiewski P, Wazny K, et al. GATA3: a multispecific but potentially useful marker in surgical pathology: a systematic analysis of 2500 epithelial and nonepithelial tumors. Am J Surg Pathol 2014;38:13–22.

[13] Iwase K, Nagasaka A, Nagatsu I, Kiuchi K, Nagatsu T, Funahashi H, et al. Tyrosine hydroxylase indicates cell differentiation of catecholamine biosynthesis in neuroendocrine tumors. J Endocrinol Invest 1994;17:235–9.

[14] Osinga TE, Korpershoek E, de Krijger RR, Kerstens MN, Dullaart RP, Kema IP, et al. Catecholamine-synthesizing enzymes are expressed in parasympathetic head and neck paraganglioma tissue. Neuroendocrinology 2015;101:289–95.

[15] Meijer WG, Copray SC, Hollema H, Kema IP, Zwart N, Mantingh-Otter I, et al. Catecholamine-synthesizing enzymes in carcinoid tumors and pheochromocytomas. Clin Chem 2003;49:586–93.

[16] Hermann G, Konukiewitz B, Schmitt A, Perren A, Klöppel G. Hormonally defined pancreatic and duodenal neuroendocrine tumors differ in their transcription factor signatures: expression of ISL1, PDX1, NGN3, and CDX2. Virchows Arch 2011;459:147–54.

[17] Weissferdt A, Kalhor N, Liu H, Rodriguez J, Fujimoto J, Tang X, et al. Thymic neuroendocrine tumors (paraganglioma and carcinoid tumors): a comparative immunohistochemical study of 46 cases. Hum Pathol 2014;45:2463–70.

[18] El-Salhy M, Lundqvist M, Wilander E. Bronchial carcinoids and phaeochromocytomas. A comparative study with special emphasis on S-100 protein, serotonin and neuron-specific enolase (NSE) immunoreactivity. APMIS (Acta Pathol Microbiol Immunol Scand) A 1986;94:229–35.

[19] Johnson TL, Zarbo RJ, Lloyd RV, Crissman JD. Paragangliomas of the head and neck: immunohistochemical neuroendocrine and intermediate filament typing. Mod Pathol 1988;1:216–23.

[20] Achilles E, Padberg BC, Holl K, Klöppel G, Schröder S. Immunocytochemistry of paragangliomas-value of staining for S-100 protein and glial fibrillary acid protein in diagnosis and prognosis. Histopathology 1991;18:453–8.

[21] Tsuta K, Raso MG, Kalhor N, Liu DC, Wistuba II, Moran CA. Sox10-positive sustentacular cells in neuroendocrine carcinoma of the lung. Histopathology 2011;58:276–85.

[22] Burke AP, Helwig EB. Gangliocytic paraganglioma. Am J Clin Pathol 1989;92:1–9.

[23] Okubo Y, Nemoto T, Wakayama M, Tochigi N, Shinozaki M, Ishiwatari T, et al. Gangliocytic paraganglioma: a multi-institutional retrospective study in Japan. BMC Canc 2015;15. 1308-8.

[24] Orrell JM, Hales SA. Paragangliomas of the cauda equina have a distinctive cytokeratin immunophenotype. Histopathology 1992;21:479–81.

[25] Miettinen M. A simple method for generating multitissue blocks without special equipment. Appl Immunohistochem Mol Morphol 2012;20:410–2.

[26] Ordonez NG. Value of GATA3 immunostaining in the diagnosis of parathyroid tumors. Appl Immunohistochem Mol Morphol 2014;22:756–61.

[27] Mete O, Kefeli M, Çalışkan S, Asa S. GATA3 immunoreactivity expands the transcription factor profile of pituitary neuroendocrine tumors. Mod Pathol 2019;32:484–9.

[28] Kimura N, Shiga K, Kaneko K, Sugisawa C, Katabami T, Naruse M. The diagnostic dilemma of GATA3 immunhistochemistry in pheochromocytoma and paraganglioma. Endocr Pathol 2020;31:95−100.
[29] Fujino Y, Nagata Y, Ogino K, Watahiki H, Ogawa H, Saitoh Y. Nonfunctional paraganglioma of the pancreas: report of a case. Surg Today 1998;28:209−12.
[30] Ginesu GC, Barmina M, Paliogiannis P, Trombetta M, Cossu ML, Feo CF, et al. Nonfunctional paraganglioma of the head of the pancreas: a rare case report. Int J Surg Case Rep 2016;8:81−4.
[31] Moran CA, Rush W, Mena H. Primary spinal paragangliomas: a clinicopathological and immunohistochemical study of 30 cases. Histopathology 1997;31:167−73.
[32] Capper D, Jones DTW, Sill M, Hovestadt V, Schrimpf D, Sturm D, et al. DNA methylation-based classification of central nervous system tumours. Nature 2018;555:469−74.